Numerical models for the resonance behaviour of the Coulomb potential in ECE theory

Horst Eckardt

Alpha Foundation's Institute for Advanced Study (A.I.A.S),

www.aias.us, www.atomicprecision.com

HorstEck@aol.com

Abstract

In Einstein-Cartan-Evans (ECE) theory the Maxwell-Heaviside electrodynamics has been corrected to a generally covariant form. The spin connections being introduced by ECE theory lead to differential equations of forced oscillations for the potential. In this paper the Coulomb law of ECE theory is studied by numerical methods. Some analytical models are proposed and implemented by computer code which is downloadable from the web site. The results depend strongly on the assumptions made for the spin connection and charge density model. The existence of resonance frequencies and resonance enhancement of the potential are approved, showing that energy transfer from spacetime is possible. In addition to the analytical forms of the spin connections, a self-consistent scheme has been defined and implemented. This gives consistent results and can be used in further applications of the ECE Coulomb law.

1 Introduction

After the development of ECE (Einstein-Cartan-Evans) theory 0 focus has now been changed to applications and numerical simulations of key features of the theory. In particular effects which are not present in standard theory (Maxwell-Heaviside electrodynamics and special relativity) will be considered. One of the most prominent of these effects is the resonance enhancement of fields by the structure of spacetime itself. This enhancement can be utilized to obtain energy from spacetime. In recent papers by M. W. Evans 0 it has been shown that the field equations of ECE theory, considered on the level of potentials, reveal the properties of differential equations for driven oscillations. Thus the mechanism of ECE resonance enhancement can be tracked down to a well known mechanism in physics. At resonance, excess energy is transferred to the oscillating parts via the driving force. Conservation laws remain valid for the whole system. In terms of ECE theory this means that energy from spacetime itself is transduced to electromagnetic or mechanical oscillations. The "driving force" is provided by imposing a timelike or spacelike periodical structure to the system.

Aim of this paper is to present means for studying the basic resonance mechanisms. The equations have been coded and are publically available [6]. The readers are encouraged to play themselves with them to obtain an impression of the effects and the opportunities. In this article we restrict ourselves to the simplest case, the electric potential, neglecting all magnetic effects. It has been shown recently that it is possible to combine the resonance effects in this approximation with standard quantum mechanical atomic structure calculations [3]. Thus it should be possible to understand the excitation mechanism on a microscopic level. We hope that resonance effects can be specifically designed in near future.

In the next section the model is described and the differences between the analytical model and numerical models are lined out. In section 3 we present the results and discuss some prominent differences between the models.

2 Model system

We choose the generalized Coulomb law of ECE theory 0 as a model system. This connects several components of the vector and scalar potential by the spin connections of Cartan geometry. We restrict ourselves to pure electrical, time-independent interactions. The Coulomb law then reads 0

$$\underline{\nabla} \cdot \underline{E} = - \frac{\rho}{\varepsilon_0} \qquad (1)$$

with

$$\underline{E} = - \left(\underline{\nabla} + \underline{\omega} \right) \Phi \qquad (2)$$

where $\underline{E}$ is the electric field, Φ the electrical scalar potential, $\underline{\omega}$ the vector of spin connections, and ρ the charge density. Inserting eq. (2) in (1) gives

$$\nabla^2 \Phi + \underline{\omega} \cdot \underline{\nabla} \Phi + \left(\underline{\nabla} \cdot \underline{\omega} \right) \Phi = \frac{\rho}{\varepsilon_0} \qquad (3)$$

This is a linear differential equation in Φ. In standard theory there is no spin connection, and eq. (3) changes to the well-known Poisson equation of electrostatics:

$$\nabla^2 \Phi = \frac{\rho}{\varepsilon_0} \qquad (4)$$

By interpreting the charge density term in eq. (1) as an oscillatory term in space

$$\rho = \rho_0 \cos(\underline{k} \cdot \underline{r}) \qquad (5)$$

with wave number κ, eq. (3) is a differential equation for a driven oscillation. Restricting our considerations to one dimension, we obtain

$$\frac{d^2\Phi}{dx^2} + \omega \frac{d\Phi}{dx} + \frac{d\omega}{dx}\Phi = \frac{\rho_0}{\varepsilon_0}\cos(kr) \qquad (6)$$

For constant values of ω and dω/dx, this gives the well-known resonance behaviour with resonance wave number κ_0. This is text book physics. The resonance wave number **Fehler! Verweisquelle konnte nicht gefunden werden.** is given by

$$K_0 = \sqrt{\frac{d\omega}{dx} - \frac{\omega^2}{2}} \qquad (7)$$

The situation gets more complicated as soon as a more realistic ω is considered which is varying in space. Then analytical solutions are difficult to obtain, and eq. (6) has to be solved numerically. This can be done straightforwardly by handling eq. (6) as an ordinary differential equation which can be solved by an iteration scheme. This is obtained in simplest form by inserting the discretized first-order derivative operators (with increment h):

$$\frac{\Phi_{n+1} - 2\Phi_n + \Phi_{n-1}}{h^2} + \omega_n \frac{\Phi_{n+1} - \Phi_{n-1}}{2h} + \underbrace{\frac{\omega_{n+1} - \omega_{n-1}}{2h}}_{\omega_n'} \Phi_n = \rho_n \qquad (8)$$

Resolving for Φ_{n+1} gives the recurrence formula:

$$\Phi_{n+1} = \frac{1}{1 + \frac{h}{2}\omega_n}\left(-\Phi_n\left(-2 + h^2\omega_n'\right) - \Phi_{n-1}\left(1 - \frac{h}{2}\omega_n\right) + h^2\rho_n\right) \qquad (9)$$

The first two values of Φ have to be predefined, representing the initial value and its derivative. It is known from driven oscillations that the resonance behaviour does not depend on the initial values, so the choice is uncritical.

A computer program has been written which assumes different forms of ω(x) and ρ(x) and can be downloaded from the AIAS web site [4]. Some example cases are discussed in the next section.

For realistic models, it is important to use a reasonable form of the spin connection function. We can do a step in this direction by the following consideration. An electrical potential deformates the spacetime by its energy content which is the potential energy

$$W_{pot} = q\,\Phi \qquad (10)$$

for a charge q. W_{pot} is proportional to the potential itself. If we assume that the deformation is purely torsion-like, we can (to a first approximation) assume

$$\omega \sim W_{pot} \sim \Phi \qquad (11)$$

Setting

$$\omega(x) = f\,\Phi(x) \qquad (12)$$

with a constant factor f, this gives a nonlinear differential equation in Φ:

$$\frac{d^2\Phi}{dx^2} + 2f\,\Phi\,\frac{d\Phi}{dx} = \frac{\rho}{\varepsilon_0} \qquad (13)$$

or

$$\frac{d^2\Phi}{dx^2} + f\frac{d(\Phi^2)}{dx} = \frac{\rho}{\varepsilon_0} \qquad (14)$$

Discretizing this equation directly gives quadratic terms in Φ which turned out to lead to significant numerical problems. It is better to stay at eq. (9) and define a solution algorithm as follows:

1. choose a start value for Φ
2. set ω=f Φ
3. solve eq. (9)
4. if new solution differs from the old, go to step 2

This leads to a self-consistent solution for Φ. The method can also be applied for atomic structure calculations where equation (3) has to be solved to obtain the Coulomb potential from the charge density 0.

3 Results

Model 1: Analytical solution

First we study the behaviour of the analytical solution of eq. (6) which has been computed numerically from eq. (9) in order to test the computer code. We have set ε_0=1, ρ_0=1 and do not further consider physical units for reasons of simplicity. In the example we have chosen ω=0.1, ω'=2. According to eq. (7), the resonance wave number should be then κ_0=1.414. In Fig. 1 the off-resonance case κ=1 is shown. Because κ is below the resonance value, driving force (ρ) and potential (Φ) are in phase. In the resonance case (Fig. 2, κ=1.414) both are shifted by 90 degrees, and the amplitude of Φ is at maximum. In Fig. 3 we see off-resonance again in the region above resonance (κ=3), leading to a phase shift of 180 degrees between ρ and Φ.

In Fig. 4 the curve of amplitude resonance $\Phi_{max}(\kappa)$ is shown for varying values of κ. It can be seen that resonance occurs at the value predicted by eq. (7).

Model 2: Linear ω(x)

The the first non-constant ω has been chosen as a linear function:

$$\omega = 0.1*x, \qquad \omega' = 0.1$$

This gives a qualitative different resonance behaviour, beginning with a maximum peak (see example for κ=1.0 in Fig. 5). The resonance curve $\Phi_{max}(\kappa)$ shows a broad maximum at κ=0.2. (Fig. 6).

Model 3: oscillating ω

Making ω an oscillating function

$$\omega = \sin(\kappa x)$$

leads to a type of unharmonic behaviour of Φ(x), see Fig. 7 for κ=0.6. The maxima of Φ increase continually for increasing x. We have restricted the calculation to 3 wavelengths for each value of κ. In this way a reasonable resonance curve can still be obtained (Fig. 8). The amplitudes increase indefinitely for κ→0. Therefore the curve begins at κ=0.18, not at κ=0.

Model 4: oscillating ω with decreasing ρ

So far the charge density ρ has been chosen to be harmonically oscillating. The results of Model 3 suggest to restrict the amplitude of ρ for increasing x in order to avoid an unlimited amplitude gain. We choose

$$\rho = \exp(-(0.1*\kappa x)^{2}) * \cos(\kappa x),$$

that is a Gaussian function modulated by a cosine. The result (Fig. 9) is even worse when considering the same κ as in Model 3 (κ=0.6). Correspondingly the resonance curve (Fig. 10) goes up even higher for κ→0. On the other hand, this can be a wanted behaviour, if very high Q factors are to be obtained.

Model 5: ω in proportion to decreasing ρ

Obviously the course of ω and dω/dx for increasing x values plays an important role for determining the resonance behaviour. in Model 5 we have simply chosen

$$\omega = \rho$$

with a decreasing ρ as in Model 4. Consequently the amplitude of Φ now does no more increase over all limits (Fig. 11). The resonance behaviour (not shown) is similar to Fig. 8 and Fig. 10 (resonance for for κ→0). In Fig. 12 we have plotted ω and ω'. The phase shift between both is a consequence of the cosine function in ω.

Model 6: ω = f Φ

The last model is the self-consistent calculation according to the ansatz given in eq. (12). Φ(x) for f=1, κ=1.3 is shown in Fig. 13. It can be seen that there is no homogeneous phase shift between Φ and ρ, indicating the non-linear nature of this ansatz compared to regular resonance equations. Convergence is difficult to obtain for values smaller than κ=1.3. Fig. 14 shows ω and ω'.

In Fig. 15 the convergence behaviour of Φ is presented. The most upper curve is the start value of Phi with ω=0 and ω'=0. This is the solution of the Coulomb law without spin connection. The solution shows a linear increase in the region of vanishing charge density, as expected from the Poisson equation. This behaviour has changed in the converged solution, there is a constant range now. This is a hint that the occurrence of a spin connection may change the qualitative behaviour of the Coulomb law completely.

Resumé

The analytical solutions of Model 1 illustrate vividly what is possible with modelling of the ECE Coulomb law. With different spin connections a large number of possibilities becomes available. A small part of them has been presented in this paper. Sometimes the solution diverges if an indefinitely expanding charge density in space is assumed. This is probably no realistic choice because the charge density of atoms is bound to the atomic volume, and in solids one would typically restrict the volume to the unit cell of the crystal lattice.

The most interesting procedure is to derive the spin connection from other physical quantitites like the potential itself, as was presented in this paper. This method can be transferred to extended computing environments like atomic and molecular structure programs where a new type of atomic excitations can be studied.

4 Acknowledgements

The AIAS members, in particular Myron W. Evans, are thanked for many interesting discussions.

5 References

[1] M. W. Evans, Generally Covariant Unified Field Theory (Abramis, 2005, softback), volume one. Ibid., vol. 2 in press, vol. 3 in preparation (preprints of vols. 2 and 3 available on www.aias.us and www.atomicprecision.com

[2] M. W. Evans, preprint 52: Resonance Solutions of the ECE Field Equations, on www.aias.us and www.atomicprecision.com

[3] M. W. Evans, preprint 59: The Resonant Coulomb Law from ECE theory: Application to the Hydrogen Atom, on www.aias.us and www.atomicprecision.com

[4] H. Eckardt: Numerical Solutions for the Resonance Equations of ECE Theory, on www.aias.us and www.atomicprecision.com

[5] J. B. Marion, S. T. Thornton, Classcial Dynamics of Particles ans Systems (Saunders College Publishing, Fort Worth, Philadelphia), fourth edition 1995, pp. 125-131

[6] H. Eckardt: Code for Paper “Numerical models for ECE resonance behaviour of the Coulomb potential”, on www.aias.us and www.atomicprecision.com

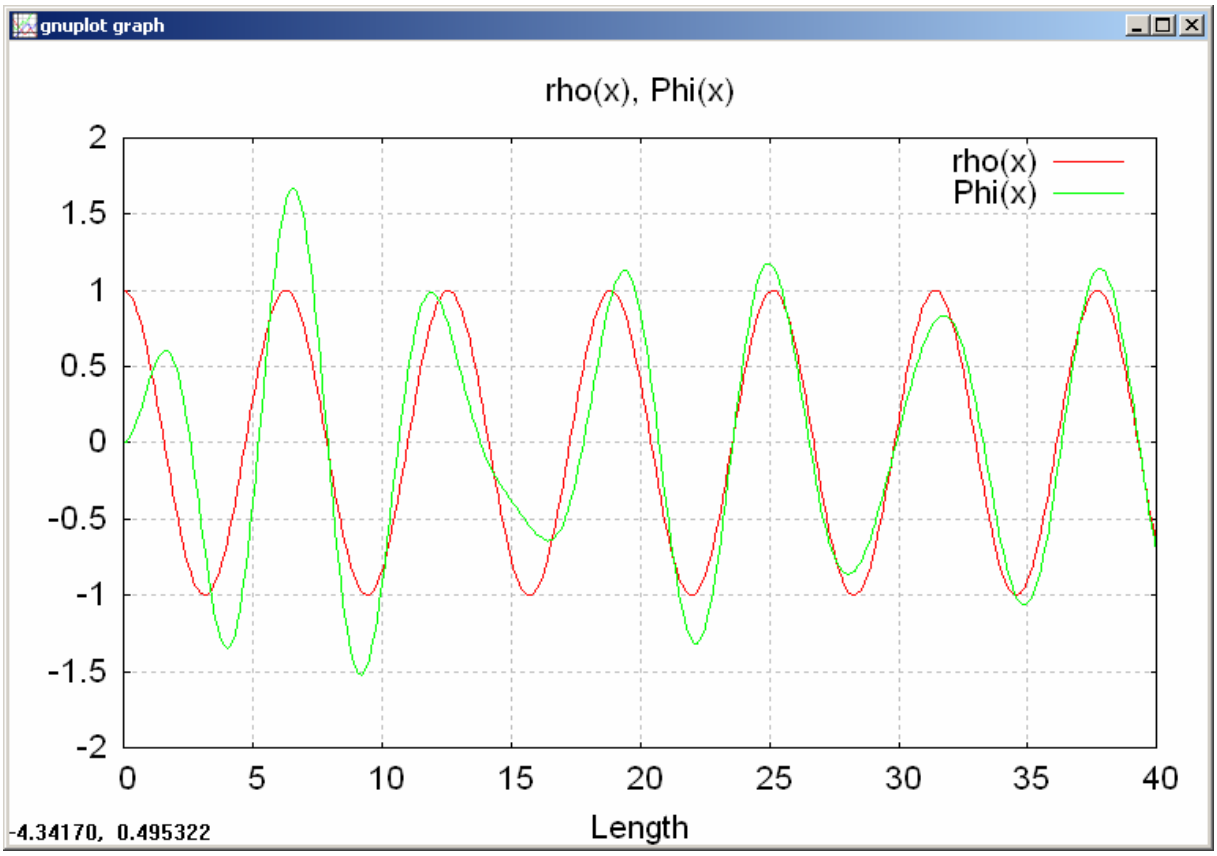

Fig. 1. Model 1: Off-resonance (κ=1.0)

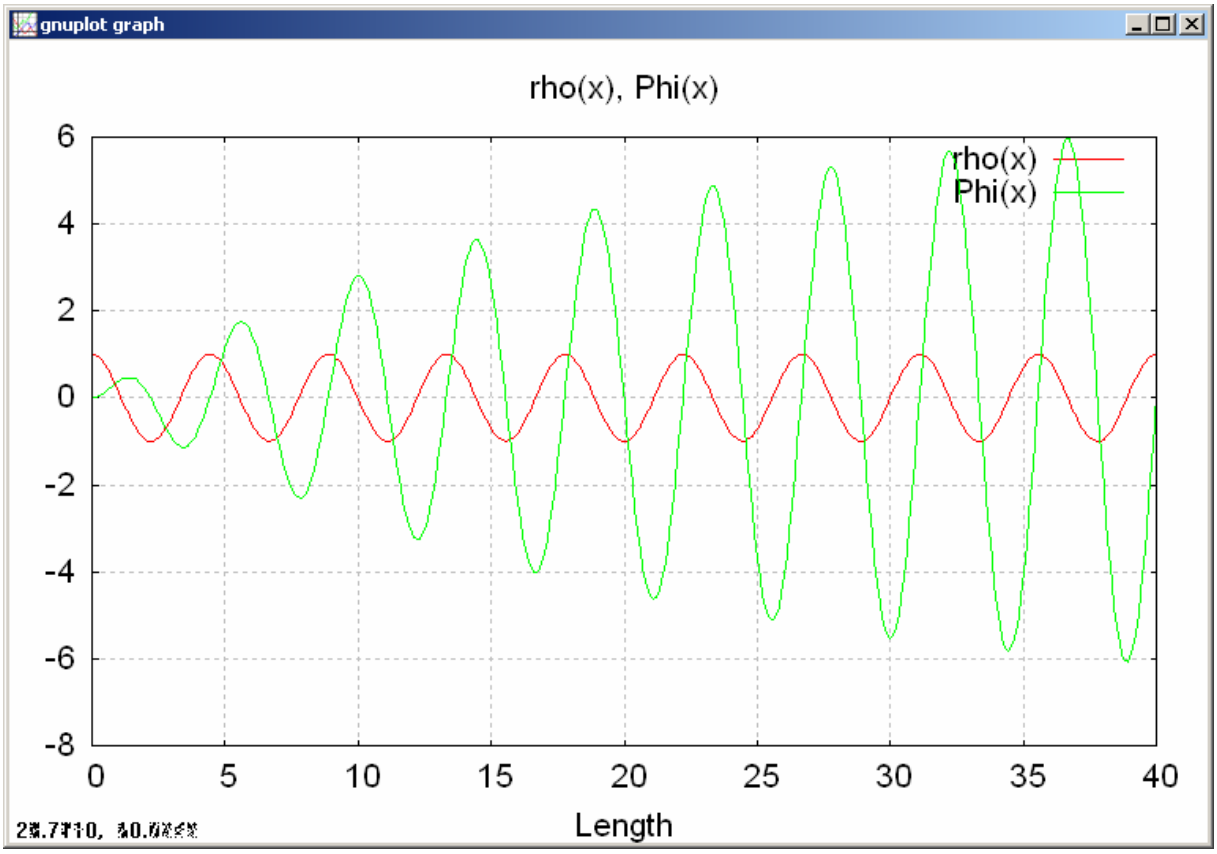

Fig. 2. Model 1: Resonance (κ=1.414)

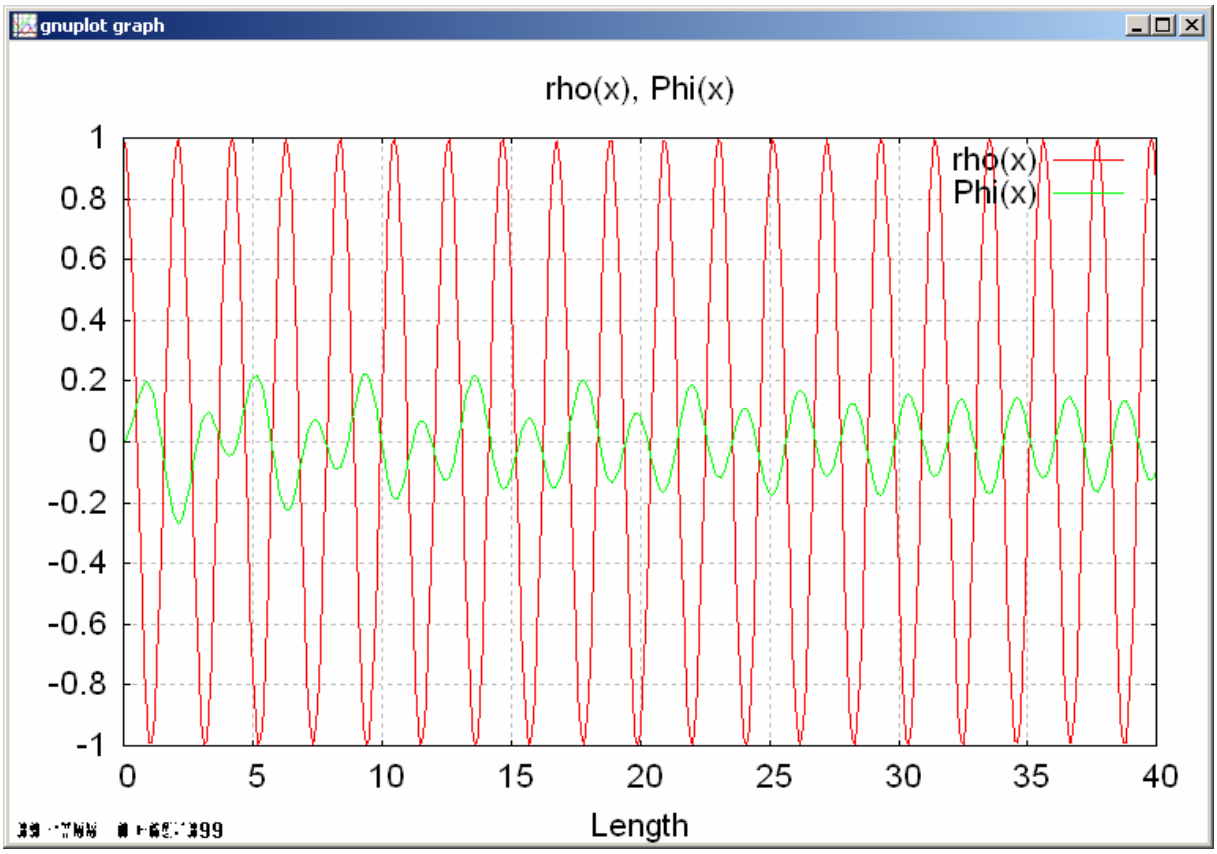

Fig. 3. Model 1: Off-resonance (κ=3.0)

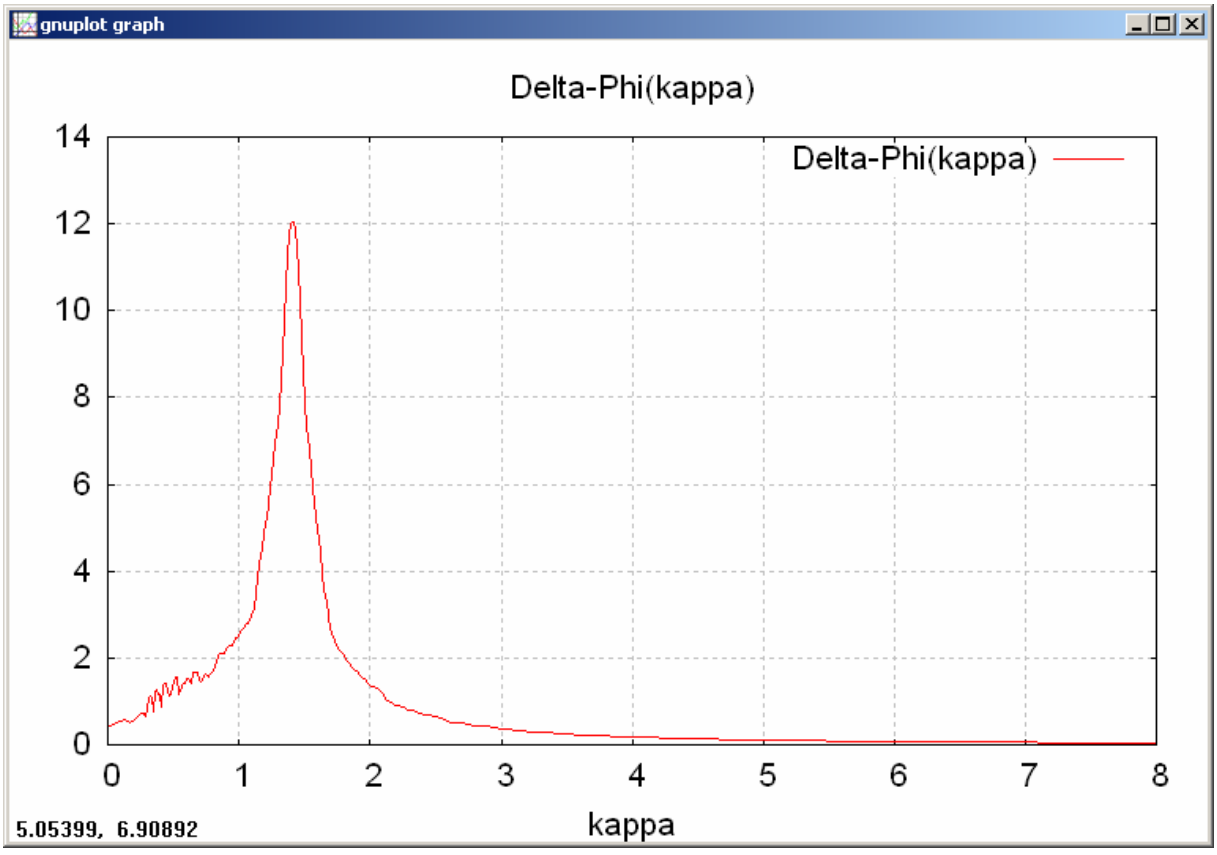

Fig. 4. Model 1: Amplitude resonance curve $\Phi_{max}(\kappa)$

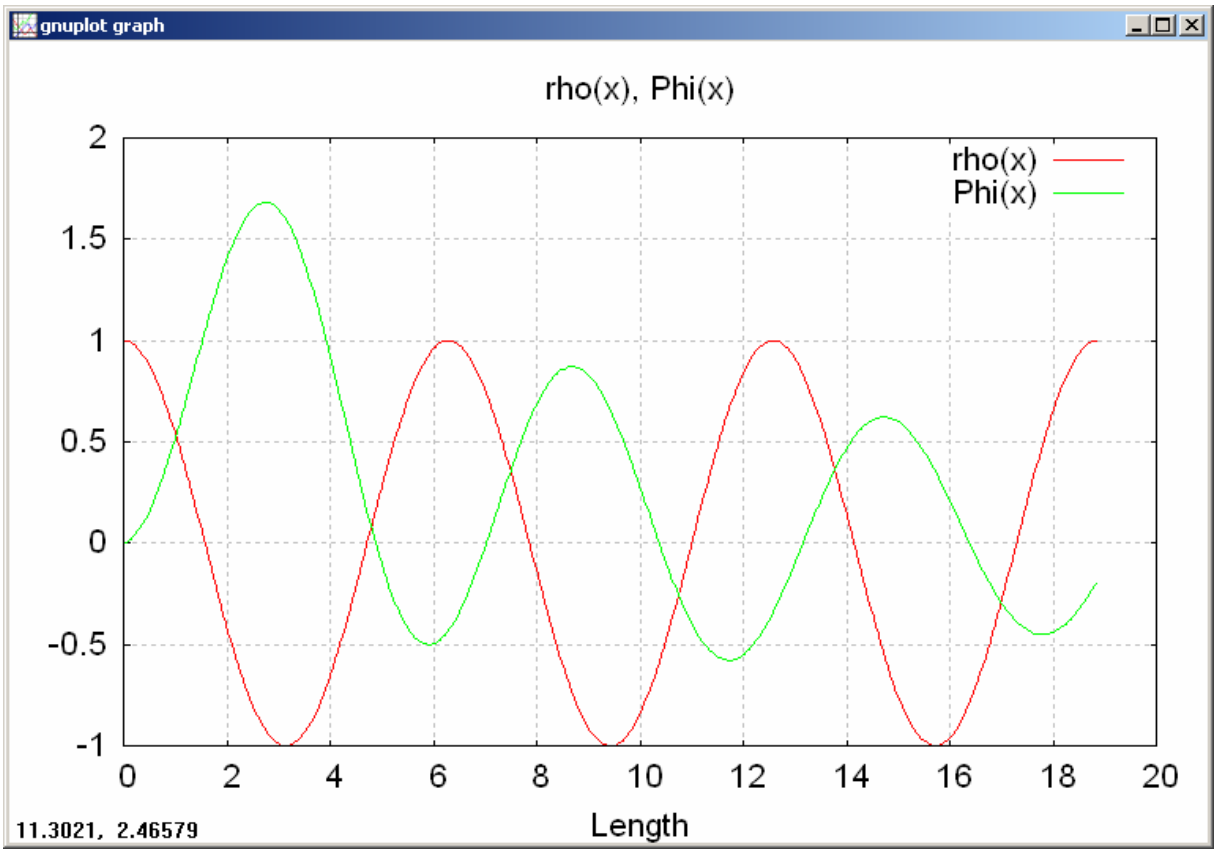

Fig. 5. Model 2: Amplitudes near to resonance

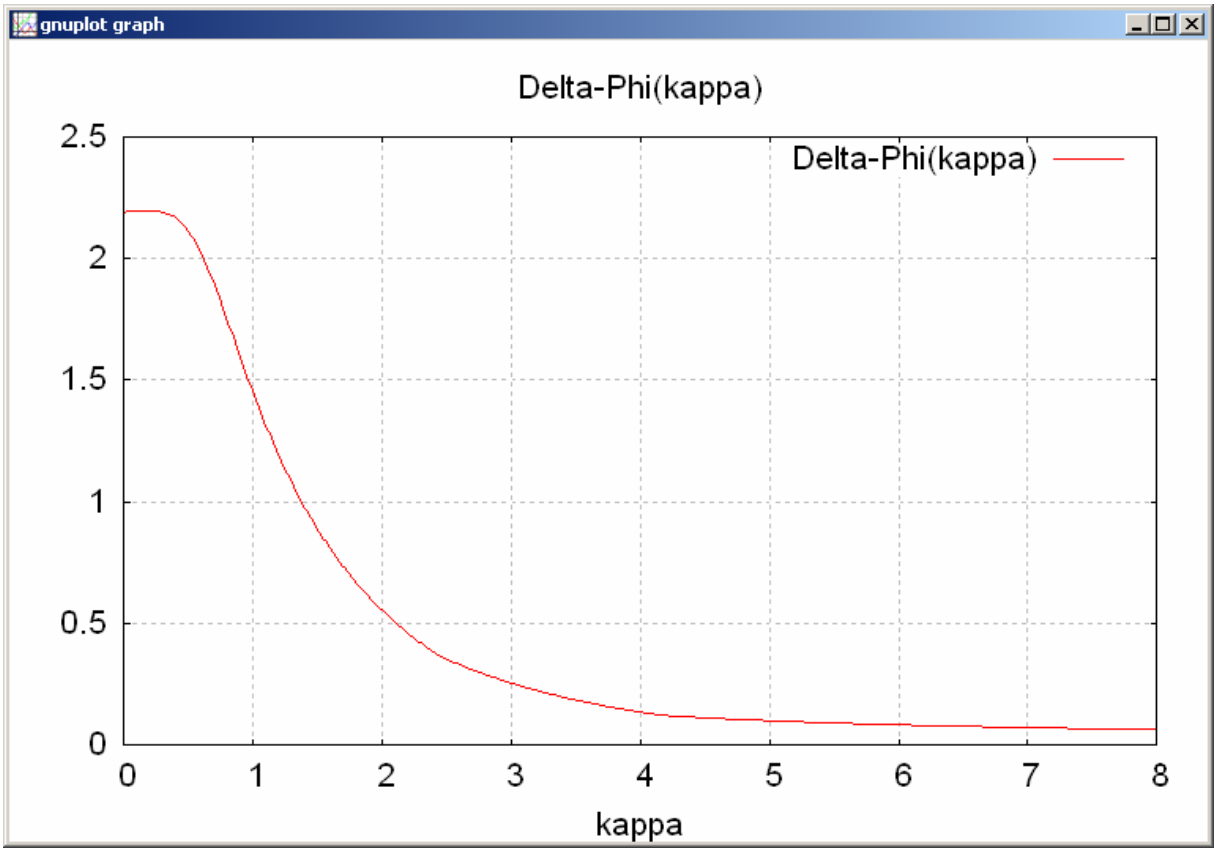

Fig. 6. Model 2: Amplitude resonance curve $\Phi_{max}(\kappa)$

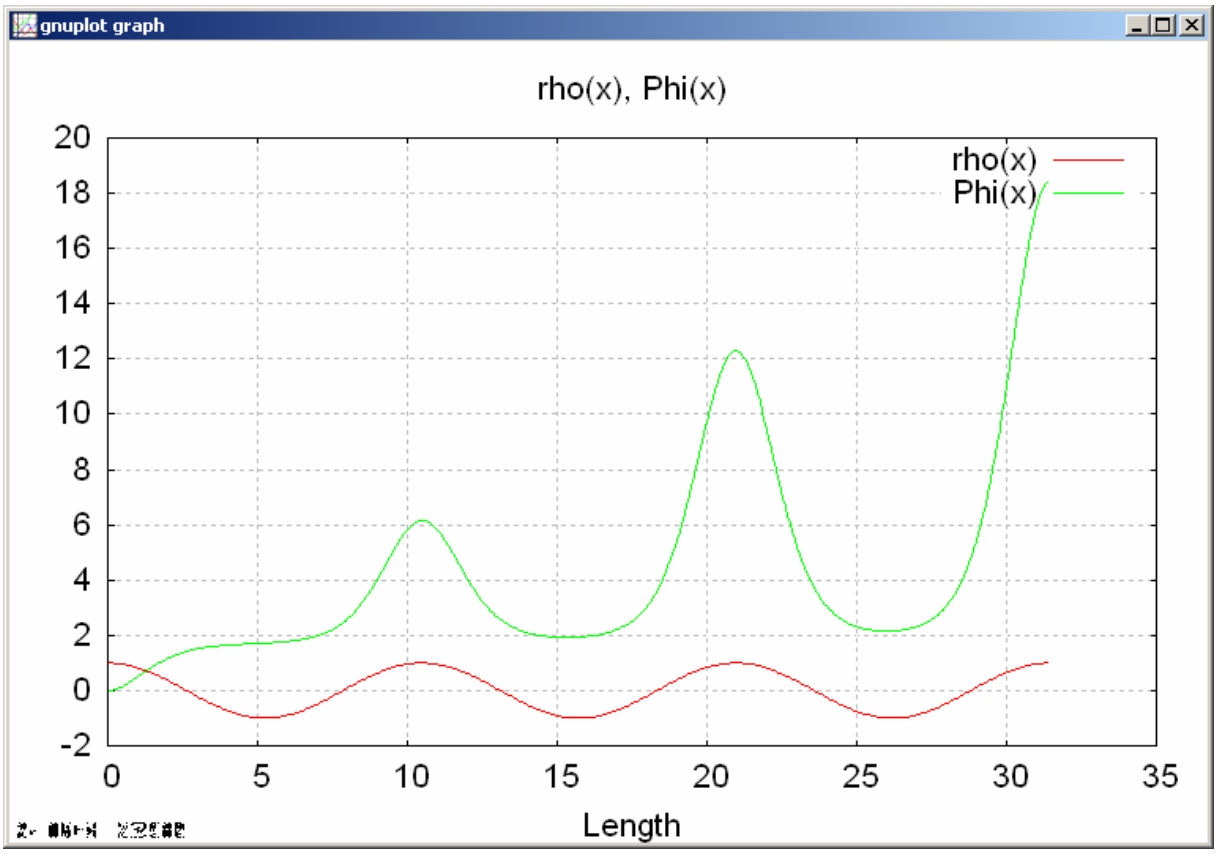

Fig. 7. Model 3: Amplitudes near to resonance

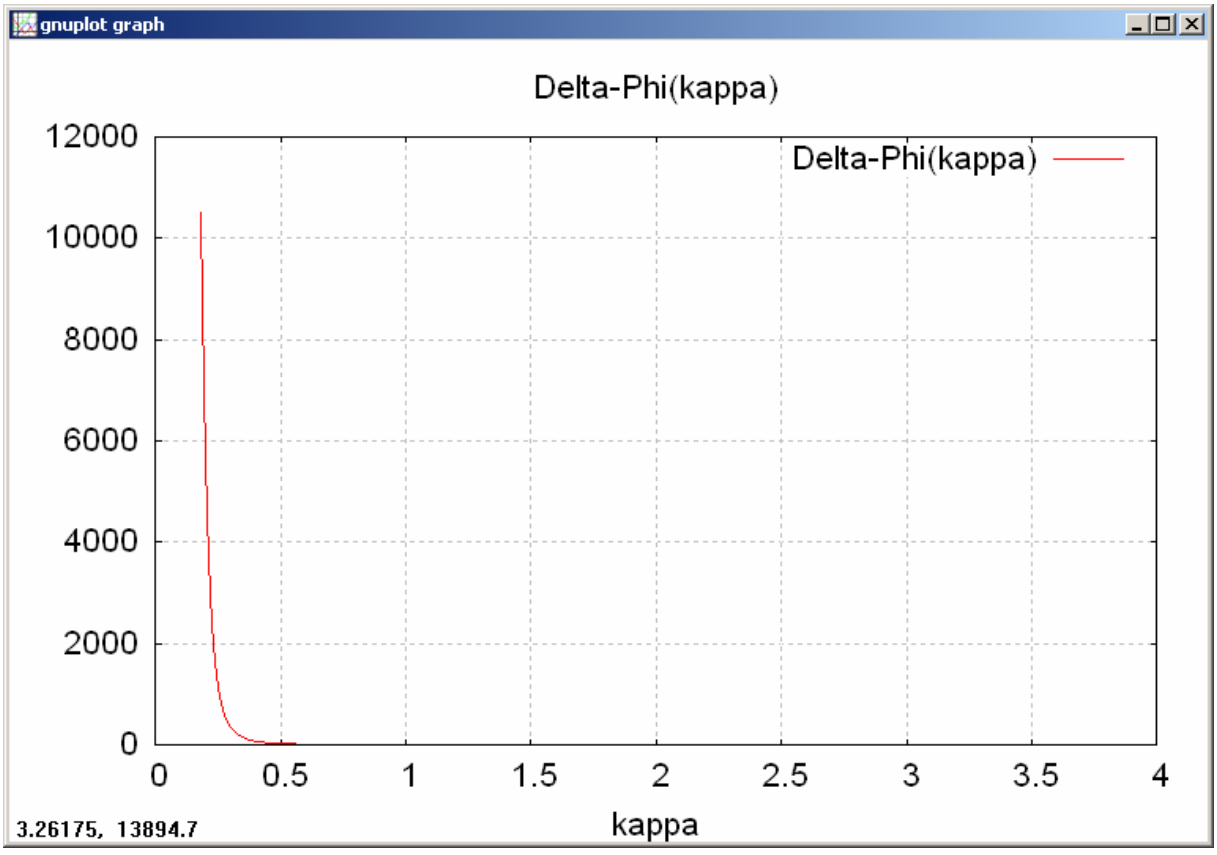

Fig. 8. Model 3: Amplitude resonance curve $\Phi_{max}(\kappa)$

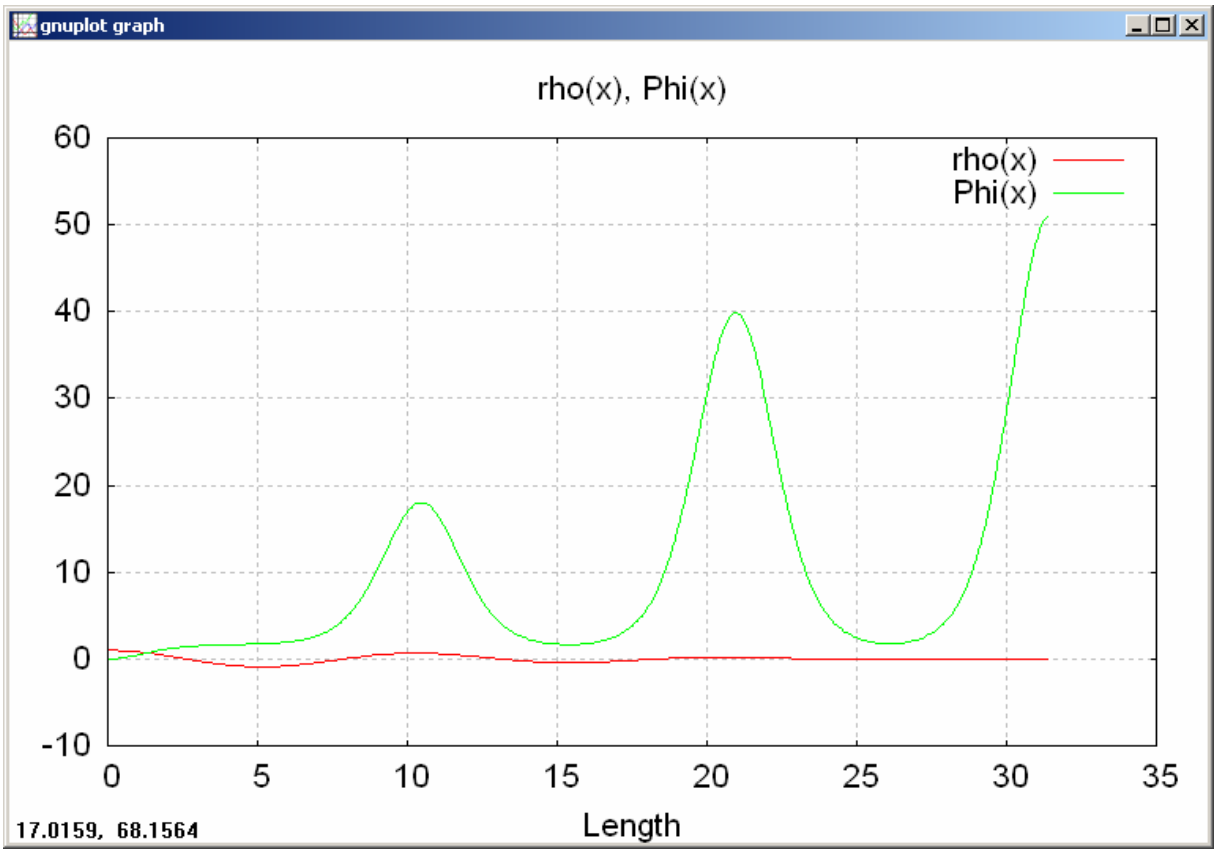

Fig. 9. Model 4: Amplitudes near to resonance

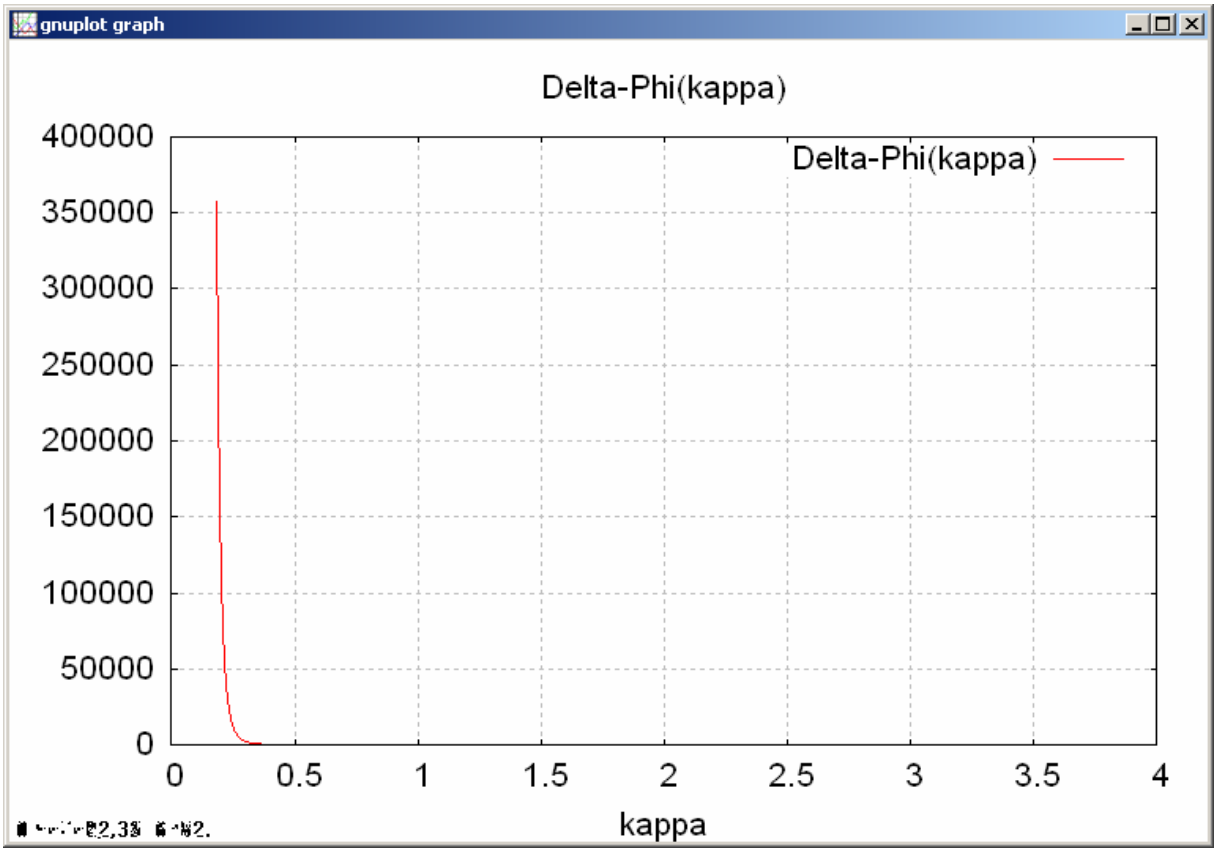

Fig. 10. Model 4: Amplitude resonance curve $\Phi_{max}(\kappa)$

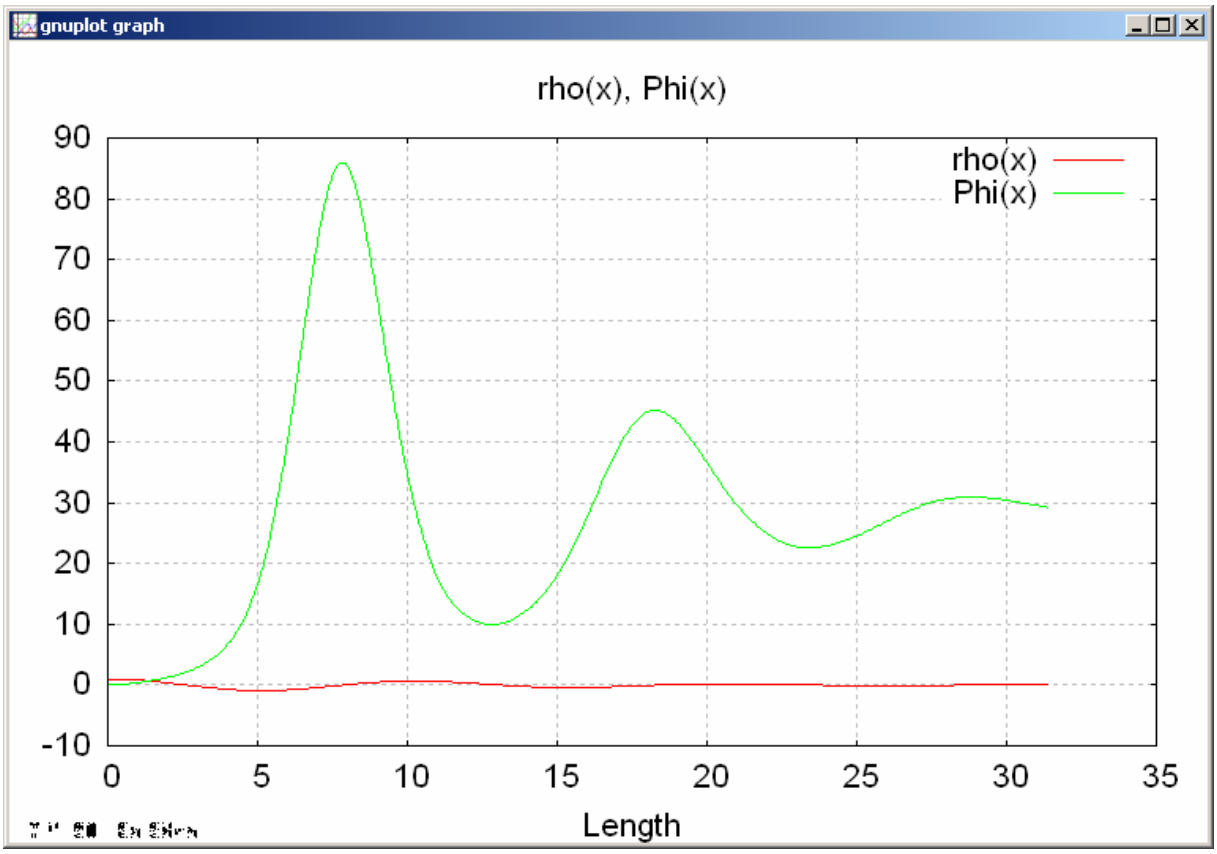

Fig. 11. Model 5: Amplitudes near to resonance

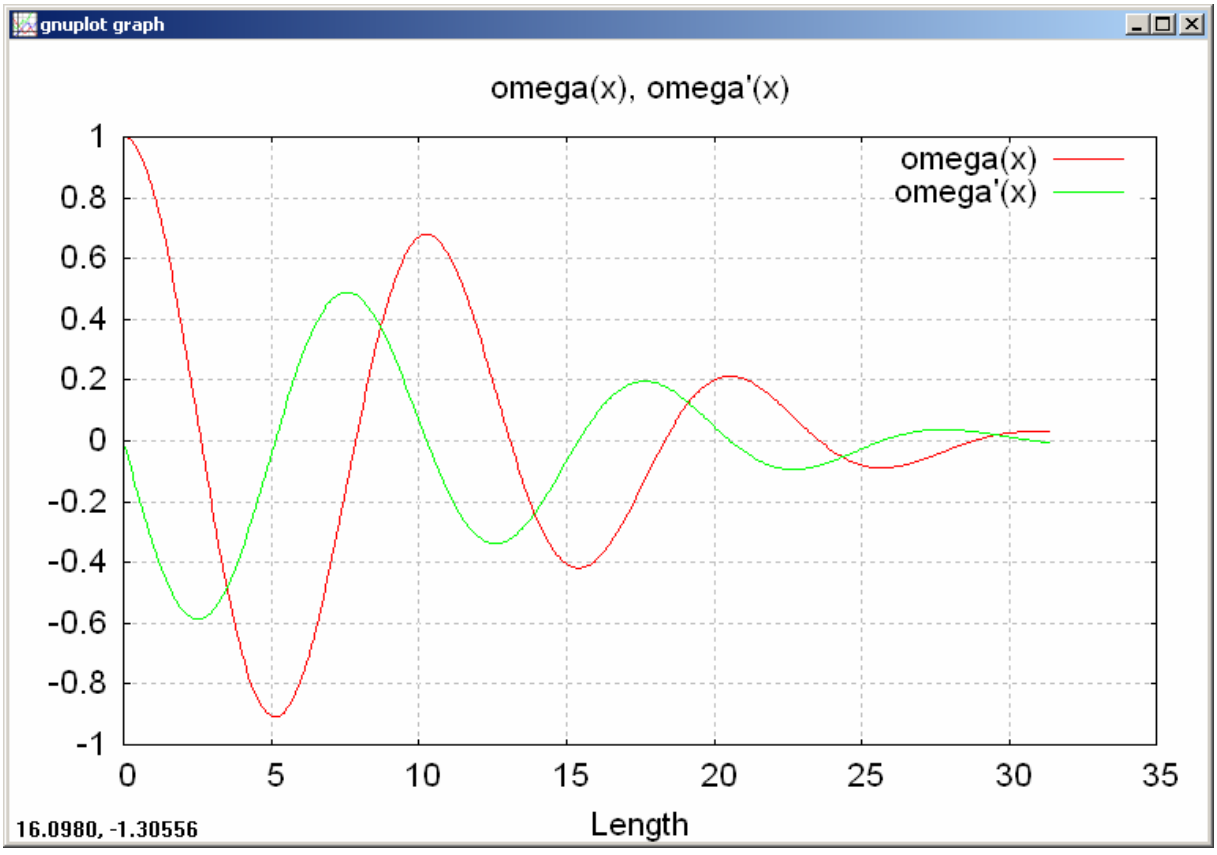

Fig. 12. Model 5: ω (in proportion to ρ) and ω’

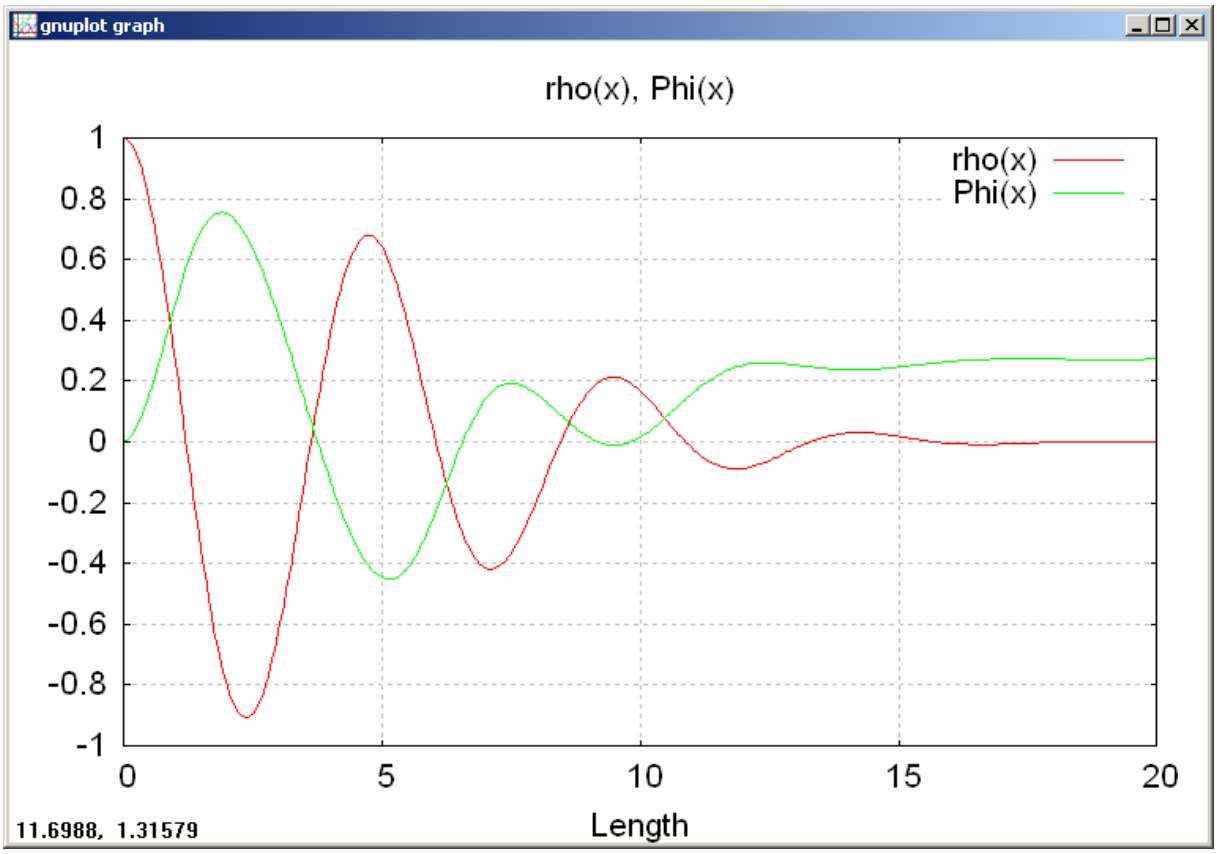

Fig. 13. Model 6: Amplitudes near to resonance

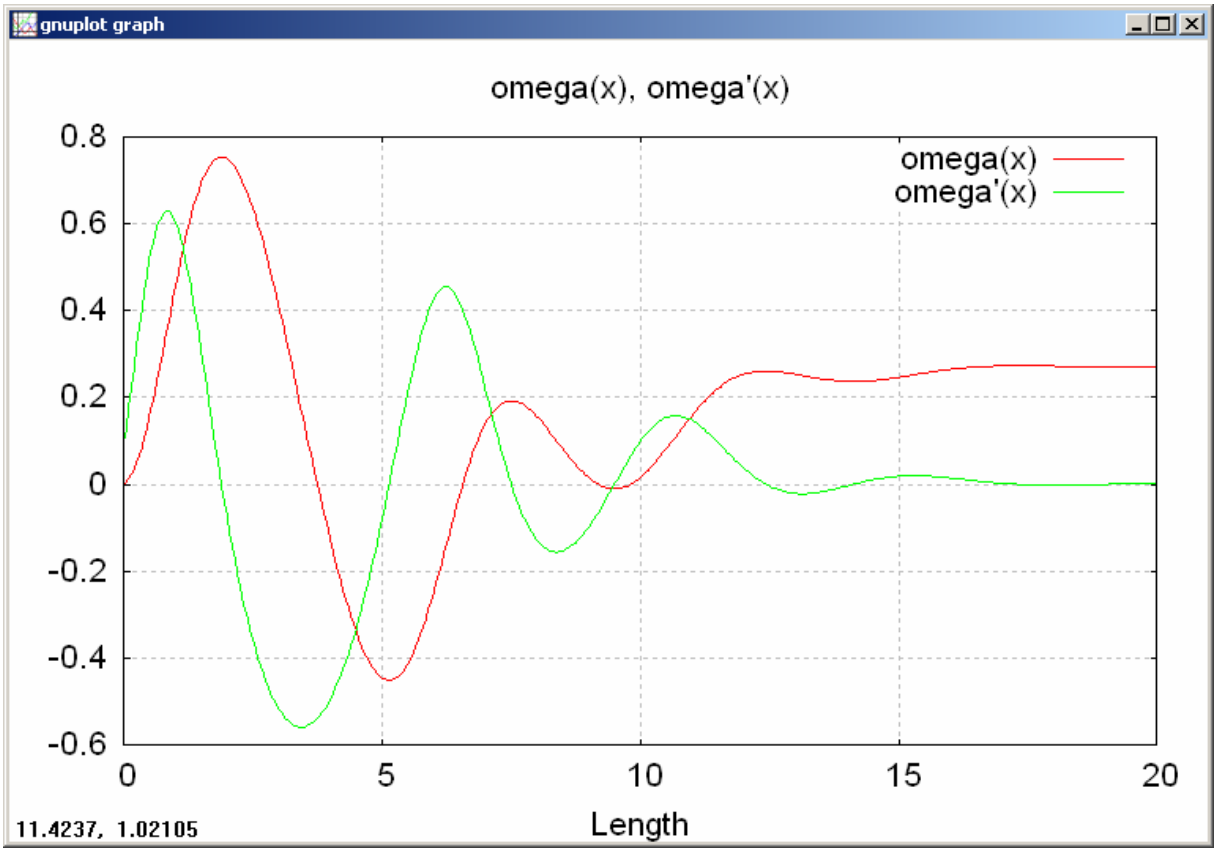

Fig. 14. Model 6: ω (in proportion to Φ) and ω’

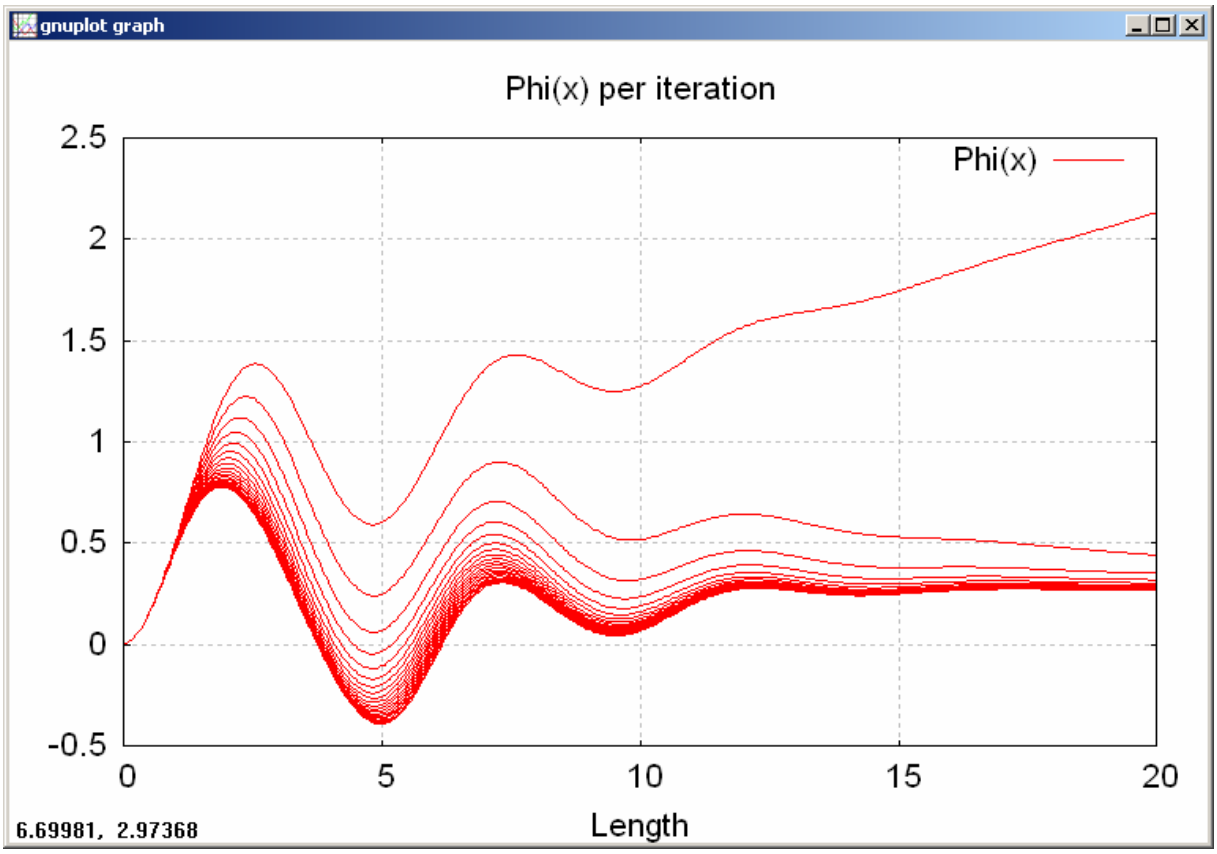

Fig. 15. Model 6: convergence behaviour of Φ(x)